JOURNAL OF APPLIED ELECTROCHEMISTRY 14 (1984) 357–366

Applications of porous flow through electrodes. II. Hydrogen evolution and metal ion removal at packed metal wool electrodes

B. G. ATEYA*, A. A. ATEYA‡, M. E. EL-SHAKRE

Chemistry Department, Faculty of Science, Cairo University, Cairo, Egypt

Received 29 March 1983, revised 2 July 1983

Packed metal wool electrodes have been used for producing hydrogen electrolytically and for removal of Cu^{2+} ions from a flowing electrolyte stream. Current–potential relations for the two reactions were measured under various operating conditions. The polarization behaviour of the packed wool electrodes has been characterised and interpreted. The effects of pore electrolyte resistance and bed thickness on the polarization of the hydrogen evolution reaction were evaluated and interpreted in terms of an existing model. The effect of the generated gas bubbles on the pore electrolyte resistance is the underlying reason for the measured excessive ohmic potential drops. It has been shown that wool-packed electrodes perform better than, or at least as well as, particle-packed electrodes (turnings, wirelets, small cylinders). The weight of metal wool needed to achieve these results is only about 10% of the weight of the metal particles. The mass transfer at the packed wool electrode has been analysed.

Nomenclature

a	Geometrical cross-sectional area of the electrode, cm^2
b	$RT/F = 0.0256$ V at 25° C
C_L, C_0	Reactant concentration at the outlet and inlet, respectively, mol cm^{-3}
d_{app}	Density of the packed bed, $cm^3 g^{-1}$
D	Diffusion coefficient of reactant, $cm^2 s^{-1}$
E_L, E_0	Electrode potential at the outlet face and entry face, respectively, V
f	Conversion efficiency, i_{L2}/i_{L1}
F	Faraday's constant, 96487 C mol^{-1}
i	Current density, A cm^{-2}
$\bar{k}_m$	Average empirical mass transfer coefficient, cm s^{-1} (Equation 4)
i_{L1}	Maximum obtainable limiting current, A cm^{-2} (Equation 3)
i_{L2}	Experimentally measured limiting current, A cm^{-2}
i_0	Exchange current density of the electrode reaction, A cm^{-2} of true surface area
I_0	Effective exchange current density of the packed bed, A cm^{-2} of geometrical cross-sectional area of the bed (Equation 11).
L	Bed thickness, cm
n	Number of electrons
Nu	Nusselt number $Nu = \bar{k}_m/DS$, dimensionless
Pe	Peclet number $Pe = V/DS$
q	Tortuosity
Q	Electrolyte volume flow rate, $cm^3 s^{-1}$
R	Average pore radius, cm (Equation 7)
Re	Reynold's number, $Re = V/Sv$
S	Specific surface area of bed, $cm^2 cm^{-3}$
V	Electrolyte flow speed, $V = Q/a$ cm s^{-1}
η_L, η_0	Polarization at the exit and entry faces, respectively, of the electrode
θ	Porosity
ϕ	Dimensionless group (Equation 6)
ρ	Electrolyte resistivity, ohm cm
ρ_{eff}	Effective pore electrolyte resistivity, $\rho_{eff} = \rho q/\theta$
ν	Kinematic viscosity, $cm^2 s^{-1}$

* Present address: Chemistry Department, Faculty of Science, University of the United Arab Emirates, Al-Ain, Abu Dhabi.
‡ Permanent address: El-Nasr Fertilizer Factories (SEMADCO), Central Laboratories, Talkha, Egypt.

0021–891X/84 $03.00 + .12

1. Introduction

There is currently a growing interest in the use of packed bed flow-through electrodes for performing many electrochemical processes. Two recent reviews on this subject have been published [1, 2]. Of particular interest is the use of this electrode system for removal of trace metal and cyanide ions from waste water streams [3, 4], charging and discharging of redox batteries for load-levelling applications [5, 6], organic and inorganic electrosyntheses and gas evolution reactions [7]. These electrodes can be operated in either fluidized or restrained modes. Each operational mode possesses some advantages and suffers from some inherent limitations. Thus, whereas fluidized bed electrodes suffer from the problems of interparticle electrical contact they require much lower-pressures to circulate the electrolyte through them. On the other hand restrained beds have no contact problem but require excessive pressures for electrolyte circulation and are subject to large values of ohmic potential drop through the pore electrolyte. This has an adverse effect on the polarization (power loss) at the electrode.

Packed metal wool electrodes seem to possess some of the advantages of both systems i.e. good electrical contact (low bed resistance) and much less resistance to electrolyte flow. They offer other advantages:

i. They can be manufactured to various specific surface areas ($cm^2\ g^{-1}$)

ii. They are rather flexible for packing, and

iii. The metal inventory needed to fill a certain electrode volume is much less in the form of wool than in the form of particles (spheres, turnings, etc.). Despite that, a packed bed of metal wool can be of higher specific surface area ($cm^2\ cm^{-3}$) than a corresponding packed bed of particles. It remains to be tested whether packed metal wool electrodes would, indeed, perform better than packed particulate electrodes.

The objective of this work is to investigate the behaviour of restrained packed-bed electrodes of metal (Cu and Ag) wool. Current–potential relations were measured, under various operating conditions for two important reactions, namely, hydrogen evolution and removal of Cu^{2+} ions from an acid solution. The results were analysed with a view to determining the sources of polarization loss. Comparison was also made between wool-packed and particle-packed beds.

2. Experimental details

Details of the experimental techniques, flow cell and circuitry have been reported elsewhere [8, 9] along with details of the calculations of tortuosity and specific surface areas of the different packing materials. SEM micrographs of the Ag and Cu wools have been reported by Ateya and El-Shakre [9]. Table 1 lists the relevant specifications of the various packed bed electrodes. Two $Hg/Hg_2SO_4/H_2SO_4$ reference electrodes ($E^0 = 0.615$ V (NHE) at 25° C.) were used for measuring the potentials at the entry and exit faces of the electrodes, the potentials being reported vs NHE.

Table 1. Specifications of the various packed bed electrodes

Number	*Type*	d_{app} ($g\ cm^{-3}$)	θ	q	S ($cm^2\ cm^{-3}$)
1	Cu wool	0.56	0.94	1.23	48
2	2/3 compressed[a] Ag wool	1.89	0.80	–	228
3	Ag wool	0.63	0.94	1.12	76
4	Cu wirelets	1.78	0.80	1.32	48
5	Cu cylinders	6.72	0.22	1.80	39
6	Cu turnings	3.03	0.64	1.60	–

[a] This electrode had the same weight of Ag wool as # 3 but packed in only 1/3 of the volume; the remaining 2/3 of electrode space was filled with glass beads.

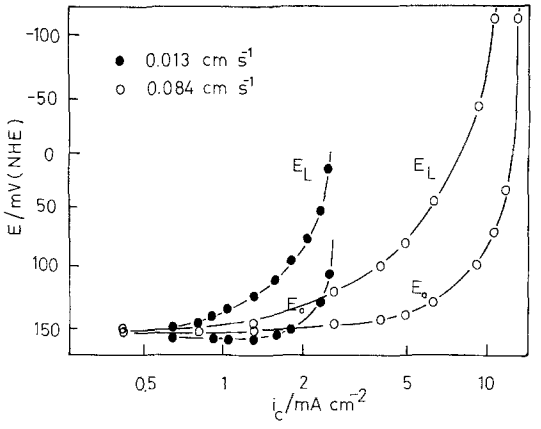

Fig. 1. Effect of electrolyte flow speed on the current–potential relations for the removal of Cu^{2+} ions. Electrolyte 0.001 mol dm^{-3} $CuSO_4$ in 3 mol dm^{-3} H_2SO_4, Electrode # 1.

3. Result and discussion

3.1. *Removal of copper ions*

Fig. 1 illustrates the effect of electrolyte flow speed on the current–potential relations at a copper wool electrode. At a certain flow speed, an increase in current increases the potential at both the entry (E_0) and exit (E_L) faces of the electrode; the increase in E_L being much greater than in E_0.

The difference between E_L and E_0 is the ohmic potential drop through the pore electrolyte. Its magnitude increases with current, electrode thickness and pore electrolyte resistance (cf. under hydrogen evolution).

At the same value of E_L, the current increases with increase in flow speed. This is characteristic of diffusion-limited reactions. The figure shows a well-defined limiting current, the magnitude of which increases with flow speed.

The change in electrolyte concentration upon passing once through the electrode is given by

$$i = nFV(C_0 - C_L) \tag{1}$$

which leads to

$$C_L/C_0 = 1 - i/i_{L1} \tag{2}$$

where C_L and C_0 are the outlet and inlet reactant concentrations, respectively; i is the current supported by the electrode reaction and i_{L1} is the maximum obtainable limiting current, given by

$$i_{L1} = nFVC_0 \tag{3}$$

which is the limiting current when the reactant is consumed entirely, i.e. $C_L = 0$. If there are internal mass transfer restrictions, the experimentally measured limiting current i_{L2} becomes less than i_{L1}. The ratio $f = i_{L2}/i_{L1}$ determines the conversion efficiency. In view of Equation 1, f is defined as the relative decrease in reactant concentration upon passing once through the electrode at sufficiently high polarization, i.e. under limiting current conditions.

The dependence of the conversion efficiency on the structural parameters of the electrode and the transport properties of the electrolyte is an important factor for design purposes. There are two approaches for obtaining such relations. The first approach is through the use of empirical mass transfer coefficients. Thus Equation 1 becomes

$$C_L/C_0 = \exp(-\bar{k}_m SL/V) \tag{4}$$

and therefore

$$f = 1 - \exp(-\bar{k}_m SL/V) \tag{5}$$

where $\bar{k}_m$ is the average mass transfer coefficient between the bed and flowing electrolyte (averaged over the entire bed thickness) and S is the specific surface area of the packed bed.

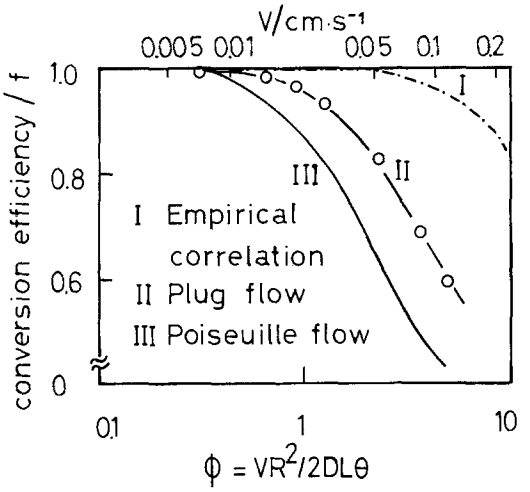

Fig. 2. Comparison of measured and calculated efficiency curves for a packed Cu wool electrode. The theoretical curves were calculated using: I – The empirical Wilson and Geankoplis correlation, II and III – solutions for plug and Poiseuille flow regimes, respectively, and $D_{Cu^{2+}} = 7.5 \times 10^{-6}$ cm^2 s^{-1} [15].

In the second approach, one uses the analytical solutions obtainable for a simplified pore geometry and then modifies them to take into account porosity and tortuosity effects [10]. A dimensionless group

$$\phi = VR^2/2DL\theta \tag{6}$$

was found to determine the efficiency (for a certain flow regime) where R is the equivalent pore radius which is related to the specific surface area of the packed bed by

$$R = 2\theta/S \tag{7}$$

Alternatively ϕ can be expressed in terms of S by

$$\phi = 2V\theta/DLS^2 \tag{8}$$

Different relations between f and ϕ were obtained for conditions of Poiseuille or plug flow. In both cases the relations were found to be highly nonlinear. These relations have been computed by Ateya [10] for the range $\phi = 0.01$–200. It is noteworthy that these solutions take into account the variation of the mass transfer coefficient with distance through the bed.

Equation 4 is applied to the present results with the following points in mind. First, the assumption of a constant value of $\bar{k}_m$ throughout the bed is justified only in deep beds [1, 10] where the diffusional entrance region is negligible compared to the bed thickness [11]. This was shown to correspond to $f \simeq 1$ [10]. Second, there are considerable discrepancies between the existing mass transfer correlations [12, 13]. In any event, none of these correlations were obtained for wool-like packings (see SEM in Reference 9) or at such a high porosity $\theta = 0.94$, and only one, by Wilson and Geankoplis [14], extends to sufficiently low Reynold's numbers of the order of the values encountered in the present work ($Re < 0.25$). This correlation is of the form [1, 14]

$$\theta . Nu = 1.09 Pe^{1/3} \tag{9}$$

where Nu and Pe are the Nusselt and Peclet numbers, respectively, expressed in terms of specific surface area S.

Fig. 2 shows a comparison of the measured efficiency curves with those predicted using: I – the empirical mass transfer correlations of Wilson and Geankoplis [14] and II and III – the analytical solutions for plug and Poiseuille flow regimes, respectively. Clearly, the Poiseuille flow solution predicts lower efficiencies while the empirical correlation predicts much higher efficiencies. (It requires about a three-fold decrease in $\bar{k}_m$ for Curve I to match the experimental curve.) The plug flow correlation gives the best agreement between predicted and measured efficiency curves. It is noteworthy that there are

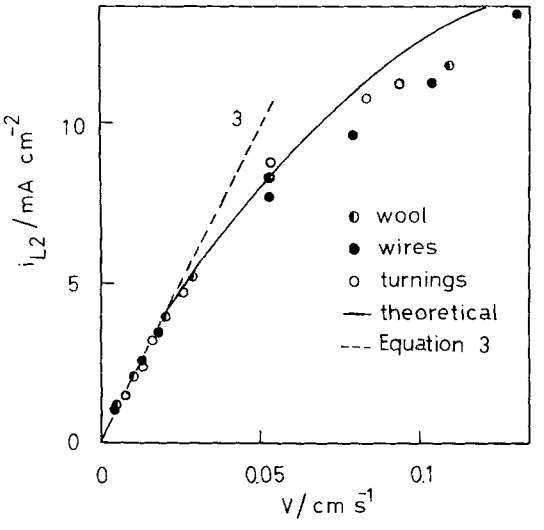

Fig. 3. Effect of electrolyte flow speed on the experimentally measured limiting current; electrodes: ◐ wool, ○ turnings and ● wirelets.

some simplifying assumptions in the model which lead to Curves II and III [10]. The bed is assumed to be a matrix of short interconnected randomly oriented pores with the mean pore radius given by Equation 7. The analytical solutions for flow through a tube (with a radius R) were obtained and then modified to take into account porosity and tortuosity effects. In spite of these assumptions, the agreement is quite good between the experimental curve and that predicted on the basis of plug flow. This indicates that the prevailing flow regime in the bed is essentially plug flow and that the variation of the local mass transfer coefficient within the bed is properly accounted for by the model equations.

Fig. 3 shows the effect of electrolyte flow speed on the limiting current for various electrodes. The figure illustrates the effect of efficiency loss at high flow rates on the measured limiting current. At low speeds the limiting current increases linearly with flow speed according to Equation 3 (while f remains constant, i.e. at $\phi < 0.4$ in Fig. 2). At higher flow speeds, the limiting current becomes progressively less than that given by Equation 3. This is a result of the progressive decrease in efficiency. The solid line in Fig. 3 is the predicted relation on the basis of the plug flow solution. This figure leads to the same conclusions as Fig. 2, but it illustrates the effect of flow speed on the limiting current more clearly.

3.2. *Hydrogen evolution*

Figs. 4 and 5 show the current–potential relations for the hydrogen evolution reaction at packed Ag and Cu wool electrodes at various flow speeds. (The dashed lines represent the predicted current–potential curves, see below.) The curves are generally similar to those obtained for Cu^{2+} deposition except for the absence of a limiting current (for hydrogen evolution). Contrary to the case of Cu^{2+} deposition, the electrolyte flow speed has no significant effect on the current–potential relations. This suggests that the reaction is not concentration dependent, hence the hydrogen ion concentration is not depleted significantly upon passing through the electrode. This can be ascertained from consideration of Equation 1. In the present work $i \leqslant 250\,\text{mA cm}^{-2}$, $V < 0.05\,\text{cm s}^{-1}$ and $C_0 = 6 \times 10^{-3}$. Therefore, the per cent of relative decrease in concentration is $(C_0 - C_L)/C_0 < 5\%$. This has been confirmed experimentally by measuring the change in acid concentration in the electrolyte upon passing through the electrode at different values of current density. A current of 44 mA cm^{-2} was impressed on electrode (# 3) at a flow speed of 0.044 cm s^{-1} and the acid concentration was determined in the effluent after about one hour. The concentration was found to decrease by only about 1%. Similar results were obtained at currents of 170 and 300 mA cm^{-2}. In all cases, concentration changes were less than 5%. This indicates that concentration variations inside the electrode and hence also concentration polarization are negligible. Therefore, it is

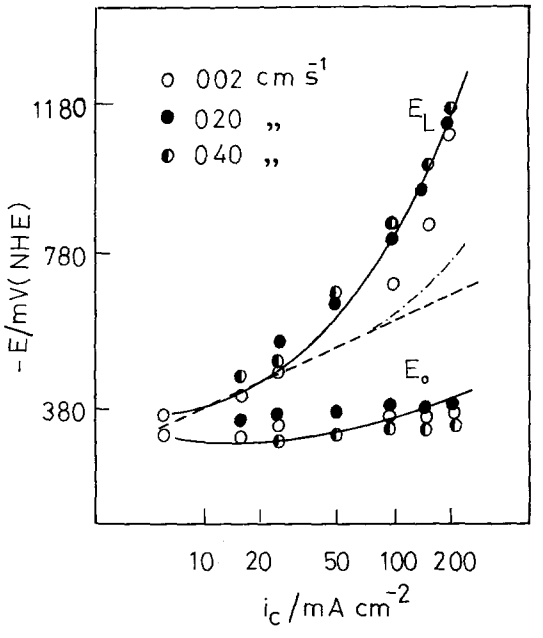

Fig. 4. Effect of electrolyte flow speed on the current–potential relations of the hydrogen evolution reaction at packed Cu wool electrodes (# 1); electrolyte: 3 mol dm^{-3} H_2SO_4. The dashed line shows the predictions of Equation 12.

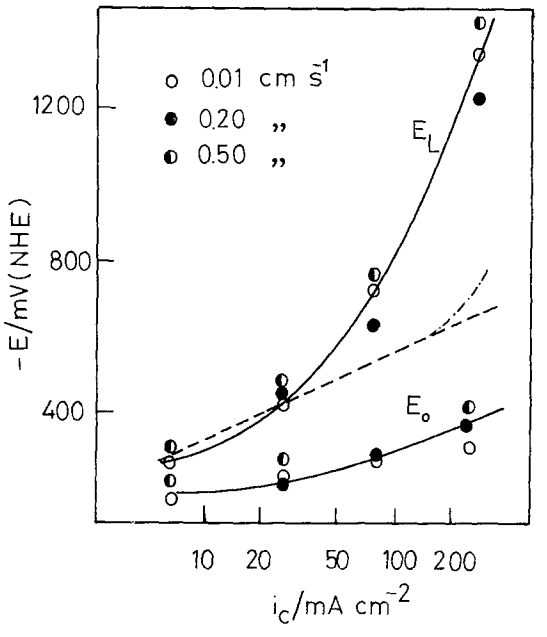

Fig. 5. Effect of electrolyte flow speed on the current–potential relations of the hydrogen evolution reaction at packed Ag wool electrodes (# 3); electrolyte: 3 mol dm^{-3} H_2SO_4. The dashed line shows the predictions of Equation 12.

concluded that the polarization (power) loss of the electrode, under the present experimental conditions, is due to both activation polarization and ohmic potential drop through the pore electrolyte. Consequently, any substantial decrease in the magnitude of one or both of these polarizations is regarded as a significant improvement in the power requirements of the process.

The literature has references to several mathematical models of porous electrodes under combined activation and ohmic control [1, 2, 4, 16–18]. These models are essentially one-dimensional and apply for simple redox reactions. No provision was made for gas evolving reactions. In order to facilitate the forthcoming discussion, and for purposes of comparison we will use the equations given by Austin and co-worker [16, 17]. At sufficiently high ohmic potential drop through the pore electrolyte, the polarization at the exit face of the electrode η_L is related to the current by

$$i = I_0 \exp(\alpha\eta_L/b) \tag{10}$$

where I_0 is the effective exchange current density given by

$$I_0 = (2i_0Sb/\alpha\rho_{\text{eff}})^{1/2} \tag{11}$$

Taking logarithms and rearranging, Equation 10 leads to

$$\eta_L = (2b/\alpha)\ln i - (b/\alpha)\ln(2i_0Sb/\alpha\rho_{\text{eff}}) \tag{12}$$

Equation 12 is a current–polarization relation with a Tafel slope of twice the normal value, i.e. it predicts an increase in polarization of 240 mV per current decade (for $\alpha = 0.5$ at 25° C). The effective exchange current density is a function of the exchange current density of the reaction on a plane surface, i_0, the specific surface area of the packed bed, S, and the effective pore electrolyte resistance ρ_{eff}. The increase in i_0 and S or the decrease in ρ_{eff} decreases the polarization, η_L; an order of magnitude increase in i_0S at constant ρ_{eff} decreases η_L by about 120 mV. It has recently been shown [9] that

gas evolution within packed bed electrodes causes significant increases in ρ_{eff} and that gas occupies significant fractions of the pore electrolyte. The trapped gas has two effects:

i. it increases ρ_{eff} by decreasing the electrolyte-filled cross-sectional area and

ii. it insulates some of the internal surface area of the packed bed from contact with the electrolyte, i.e. the effective value of S would actually be smaller than the value reported in Table 1.

Both of these effects lead to increase in η_L; this increase is accentuated as the current increases. We have measured ρ_{eff} and S and obtained values of i_0 and α from the literature [19, 20]. Therefore, we can now compare the predictions of the model and the experimental results. The dashed straight lines in Figs. 4 and 5 show the predicted current–potential relations using $i_0 = 10^{-7}$ A cm^2 for Cu, $i_0 = 3 \times 10^{-7}$ A cm^{-2} for Ag and $\alpha = 0.5$ for both [19, 20], $\rho_{eff} = 5.25$ ohm cm [9] and $b = 0.025$ V. The curvature on the dashed lines shows the effect of trapped gas on the effective pore electrolyte resistance. It was calculated using the values of ρ_{eff} measured at different rates of hydrogen evolution (see Ateya and El-Shakre [9] for the effect of current on the extent of trapping of hydrogen gas within the pores).

The agreement between the experimental results and the model predictions is at best semi-quantitiative at low currents. At higher currents there is virtually no agreement. However, upon taking account of the effect of trapped gas on the pore electrolyte resistance, the model predicts correctly the shape of the observed curves; the predicted potentials are considerably lower than those measured. It is believed that closer agreement can be obtained if it were possible to estimate the extent of surface area insulated by the trapped gas from contact with electrolyte, and take proper account of its effect on the potential (see Equation 12). It was not possible to measure the change in S with current, as was done with the pore electrolyte resistance.

3.2.1. Pore electrolyte resistance. The difference between exit and entry face potentials $\Delta E = E_L - E_0 = \eta_L - \eta_0$ is due to the ohmic potential drop through the pore electrolyte. Its magnitude increases with current, electrode thickness and pore electrolyte resistance. According to the above-mentioned model [17], the relation between η_L and η_0 is given by Equation 13 for the present condition, i.e. under ohmic control

$$\exp\left[\frac{\alpha}{2b}(\eta_L - \eta_0)\right] = \sec\left\{L\left[\frac{\alpha i_0 \rho_{eff}}{2b}\exp\left(\frac{\alpha\eta_0}{b}\right)\right]^{1/2}\right\} \tag{13}$$

This equation illustrates the effect of electrode thickness L and pore electrolyte resistivity ρ_{eff} on η_0 and $\Delta E = \eta_L - \eta_0$. Thus as L and ρ_{eff} increase, η_0 decreases while ΔE increases, and the dependence of η_0 and ΔE on L and ρ_{eff} is rather nonlinear. These features are illustrated in Fig. 6 which shows the current–potential relations measured in two electrolytes of different resistivities and equal acid concentrations under otherwise the same conditions. The electrolytes were 0.05 mol dm^{-3} H_2SO_4 ($\rho_{eff} = 52.3$ ohm cm) and 0.05 mol dm^{-3} H_2SO_4 in 1 mol dm^{-3} KCl ($\rho_{eff} = 11.8$ ohm cm). The figure shows that both E_L and ΔE are lower for the less resistive electrolyte than for the more resistive one. Consequently, it will be beneficial, in terms of ohmic potential drop within the electrode, to perform the electrolysis in electrolytes of low resistivity; this is particularly useful at higher rates.

Upon using values of i_0, S and ρ_{eff} pertinent to the present work, Equation 13 predicts much lower values of ohmic potential drop $\Delta E = \eta_L - \eta_0$ than those measured, again pointing to the serious effects of the trapped gas bubbles (see below). On the other hand, the effect of ρ_{eff} on η_L can be estimated using Equation 12. This equation predicts an increase in η_L of 120 mV for an order of magnitude increase in ρ_{eff}. For the increase in ρ_{eff} shown in Fig. 6 ($\sim 4\frac{1}{2}$ times), Equation 12 predicts an increase in η_L of 80 mV. The observed shift is of this order only at very low currents (< 5 mA cm^{-2}); it increases progressively with current, reaching several hundreds of millivolts at 20 mA cm^{-2} (see Fig. 6).

3.2.2. Bed thickness. The flexibility of the metal wool enables one to compress the same weight into a smaller volume. The following changes result from this compression:

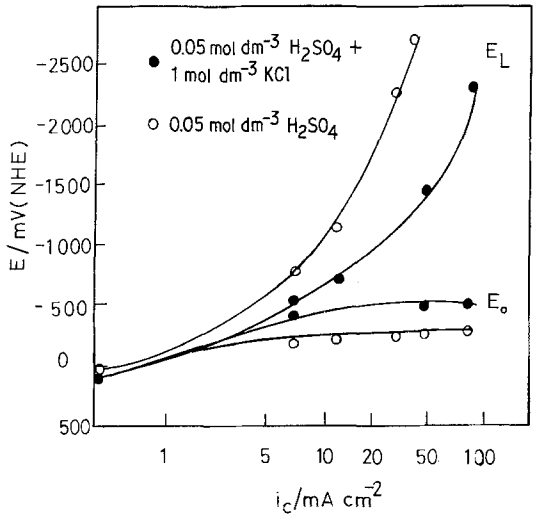

Fig. 6. Effect of electrolyte resistivity on the current–potential relations for the hydrogen evolution reaction at a Cu wool electrode (# 1).

i. the electrode thickness decreases and hence also the ohmic potential drop through the pore electrolyte (see Equation 13).

ii. The specific surface area, S (cm^2 cm^{-3}) increases proportionately resulting in a decrease in activation polarization (see Equation 12)

iii. At such high porosities, a three fold decrease in volume results in a much smaller increase in porosity (see Table 1).

Fig. 7 shows the effect of a 2/3 decrease in bed thickness on the current–potential relations of the hydrogen evolution reaction using the same weight of wool, and otherwise the same conditions. The compressed bed was only 1/3 the thickness of the uncompressed (the remainder of the electrode space was filled with glass beads). Clearly the compressed bed is polarized significantly less than the uncompressed. The polarization difference between the two cases increases with the magnitude of the current.

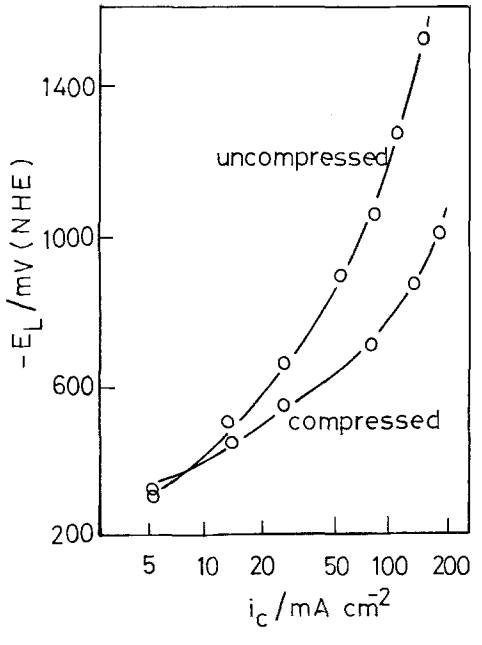

Fig. 7. Effect of 2/3 compressing of Ag wool electrode on the current–potential relations of the hydrogen evolution reaction.

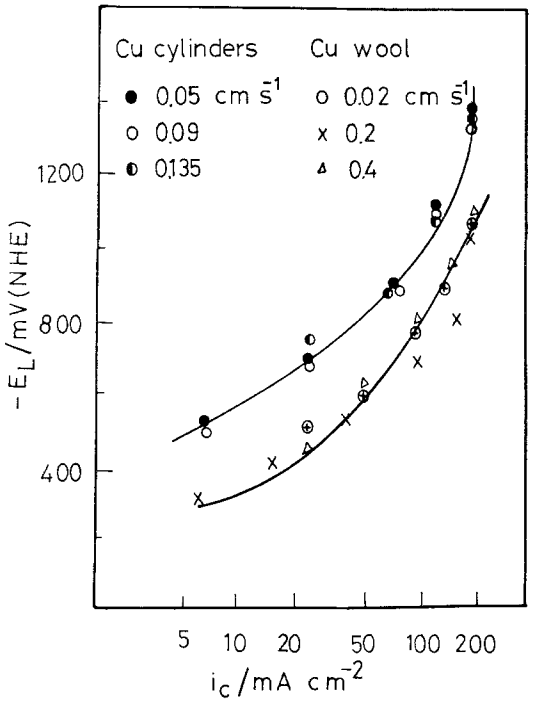

Fig. 8. Comparison of the current–potential relations of wool-packed (# 1) and particle-packed (# 5) electrodes for the hydrogen evolution reaction.

According to Equation 12, a three-fold increase in S results in about 60 mV decrease in polarization. This is much less than the observed shift particularly at high currents. Note that the compressed bed is subject to lower ohmic potential drops than the uncompressed. It is thus believed that the decrease in potential at the compressed bed is due to lower ohmic and activation polarizations.

Equations 10–13 are used here solely to illustrate the interplay of the various parameters, i.e. i_0, S, L and ρ_{eff} on the current–potential relations. The agreement between the theoretical predictions and the experimental results is only qualitative in most cases, i.e. the equations predict the direction of the change which results from the variation in a certain parameter; the measured effect is usually much greater than that predicted. The model leading to Equations 10–13 was formulated for a simple electrode reaction where no account was taken of evolving gas bubbles. The most serious difference between this model and the present experimental system is the presence (i.e. generation and retention) of gas bubbles. The electrode reaction is usually nonuniformly distributed through the bed, hence also the rate of generation of gas bubbles. Consequently, the pore electrolyte resistance increases to different extents depending on the position within the packed bed. This causes significant changes in the potential and current distributions through the bed in addition to increased ohmic potential drop through the bed due to the higher pore electrolyte resistance. It is difficult to predict the behaviour of such an electrode in a more quantitative manner since the behaviour of the gas bubbles within the packed bed is difficult to describe. A model taking into account the effect of generated bubbles on the current and potential distributions remains to be formulated and its equations solved.

3.3. *Comparison of wool and particle packings*

Figs. 8 and 9 show comparisons between wool-packed and particle-packed electrodes for the hydrogen evolution reaction (h.e.r.) and the electrodeposition of Cu^{2+} ions. The figures show that packed wool electrodes have lower or at least comparable polarization requirements as compared to packed particle electrodes. The measured polarization is the sum of activation polarization (which decreases with an increase of S) and ohmic polarization (which increases with an increase in the effective pore electrolyte

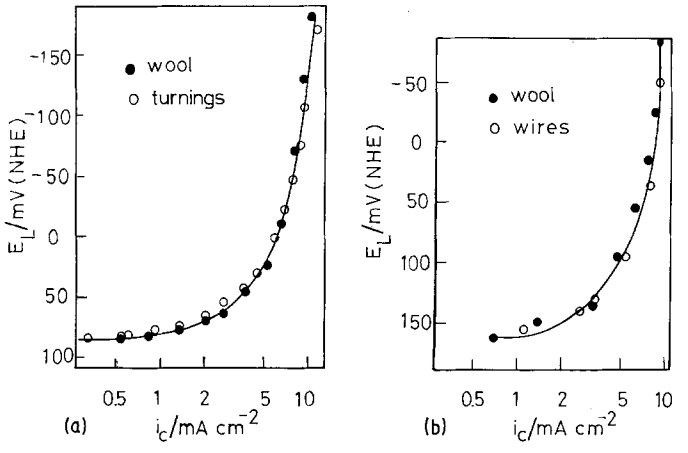

Fig. 9. (a) Comparison of the current–potential relations of wool-packed (# 1) and particles-packed (# 6) electrodes for the removal of Cu^{2+} ions. (b) Comparison of the current–potential relations of wool-packed (# 1) and particles-packed (# 4) electrodes the the removal of Cu^{2+} ions.

resistance ρ_{eff}, where $\rho_{eff} = \rho_{free} q/\theta$ where q/θ is the labyrinth factor). Thus, for the h.e.r. although the wool (# 1) and cylinder (# 5) packings have comparable values of S (i.e. comparable activation polarizations), the factor q/θ is 1.3 for (# 1) as compared to 8.9 for (# 5). Electrode # 5 must then be subject to significantly more ohmic polarization than the wool-packed bed. Similar considerations apply to the removal of Cu^{2+} ions, Fig. 9. The main advantage offered by the wool packing is that, for comparable (or better) performance, the weight of Cu in the form of wool is only about 10% of the weight of Cu in the form of particles.

References

[1] J. Newman and W. Tiedman, 'Advances in Electrochemistry and Electrochemical Engineering', Vol. 11 (edited by H. Gerischer and C. W. Tobias) Wiley, New York (1978) p. 352.
[2] R. E. Sioda and K. B. Keating, 'Electroanalytical Chemistry', Vol. 12 (edited by A. J. Bard) Dekker, New York (1982).
[3] D. T. Chin and B. Eckert, *Plat. Surf. Finish.* **10** (1976) 38.
[4] D.N. Bennion and J. Newman, *J. Appl. Electrochem.* **2** (1972) 113.
[5] M. Warshy and L. O. Wright, *J. Electrochem. Soc.* **124** (1977) 173.
[6] K. Kinoshita and S. C. Leach, *ibid.* **129** (1982) 1993.
[7] B. G. Ateya and E. S. Arafat, *ibid.* **130** (1983) 380.
[8] B. G. Ateya, E. S. Arafat and S. A. Kafafi, *J. Appl. Electrochem.* 7 (1977) 107.
[9] B. G. Ateya and M. E. El-Shakre, *ibid.* **14** (1984) 367.
[10] B. G. Ateya, *ibid.* **10** (1980) 627.
[11] B. G. Ateya, *J. Electroanal. Chem.* 77 (1977) 183.
[12] I. Colquhoun-Lee and J. Stepanek, *Chem. Eng.* **282** (1974) 108.
[13] P. S. Fedkiw, *J. Electrochem. Soc.* **128** (1981) 831.
[14] E. J. Wilson and C. J. Geankoplis, *Ind. Eng. Chem. Fund.* **5** (1966) 9.
[15] W. Eversole, H. Kindswater and J. Peterson, *J. Phys. Chem.* **46** (1942) 370.
[16] L. G. Austin, in 'Handbook of Fuel Cell Technology' (edited by C. Berger) Prentice-Hall, Englewood Cliffs, New Jersey (1968) p. 178.
[17] L. G. Austin and E. G. Gagnon, *AIChE J.* **17** (1971) 1057.
[18] J. Newman and C. Tobias, *J. Electrochem. Soc.* **109** (1962) 1183.
[19] H. Kita, 'Electrode Processes, Transactions of the 1966 Symposium' (edited by E. Yeager, H. Hoffman and E. Eisenman) The Electrochemical Society Inc., New Jersey (1967) p. 79.
[20] S. Trasatti, *J. Electroanal. Chem.* **39** (1972) 163.